

Design and Development of Quadcopter's Frame

Kaspul Anuar^{a,*}, Anita Susilawati^a, Syafri Syafri^a, Warman Fatra^a, Feblil Huda^a,
Nazaruddin Nazaruddin^a and Dedi Rosa Putra Cupu^a

^{a)} Mechanical Engineering, Universitas Riau, Indonesia

*Corresponding author: kaspul.anuar@lecturer.unri.ac.id

Paper History

Received: 09-January-2024

Received in revised form: 08-February-2024

Accepted: 30-March-2024

ABSTRACT

The purpose of this research is to obtain a design and prototype of quadcopter's frame, which be developed further as a quadcopter that capable of carrying payload of 1.5 kg with flight time of more than 20 minutes. The design begins with estimating the values of Maximum Take-Off Weight (MTOW), required thrust, propeller dimensions, and wheelbase dimensions of the quadcopter. The results show the MTOW of the quadcopter was 5 kg, with each motor requiring of 2.5 kg of thrust per arm. The wheelbase dimension was 790 mm, and the propeller diameter of 17 inches. A wheelbase dimension was utilized to develop three conceptual frame designs for the quadcopter. The three conceptual designs were selected using a decision matrix table. The selected design was calculated for its structural strength by applying a load of 2.5 kg on each motor mounting. The results show the maximum stress value of 21.17 MPa, the maximum deflection of 3.5 mm, and safety factor of 22.44. Then, the prototype of quadcopter's frame was manufactured. Therefore, the producing of prototype was measured the mass and deflection. Based on the measurements conducted, the quadcopter frame has an actual mass of 595 grams and a maximum deflection of 3.7 mm. The actual deflection value and the actual mass are close to the deflection and mass obtained from the calculation.

KEYWORDS: *Quadcopter Frame, Structural Strength, Maximum Stress.*

1.0 INTRODUCTION

Multicopter is an Unmanned Aerial Vehicle (UAV) that its lift and thrust are generated by the propulsion motor [1][2]. Generally, multicopter have more than one propulsion motor [3]. According to the number of propulsion motors, multi-

copter types can be classified into tricopter, quadcopter, and hexacopter [4]. Multicopter applications have been widely used for various purposes, both in the military and civilian sectors [5][6]. Multicopters are commonly used for photography, aerial video, and mapping/surveillance of an area [7]. One of the most commonly used types of multicopter for aerial mapping missions is the quadcopter. The quadcopter is one of the multicopter types that has four propulsion motors [8].

Recently the use of quadcopters has become increasingly for various civil purposes, such as mapping industrial forest plantations and monitoring plantation areas [7]. The development of quadcopter is expected to continue to rise, especially in Indonesia. It is supported by the presence of the growing oil palm plantation industry and industrial forest plantations [9]. Quadcopter have limitations in terms of flight time. Typically, Quadcopters are able to fly for 15 - 20 minutes with a fully charged battery [10]. The limited flight time capacity of quadcopter restricts the extent of the area that can be mapped or monitored by these devices. Therefore, if quadcopters are used for aerial mapping missions in large areas, they become less effective [11].

To enhance the flight time of quadcopters, several components need to be developed, including the battery capacity used or payload capacity, propulsion systems, and the structural frame that supports the quadcopter's payload. This research discusses the development of the quadcopter focused on the structural frame. The structural frame is designed to withstand the payload weight of 1.5 kg, supporting aerial mapping missions with a flight time capacity of more than 20 minutes.

2.0 METHODS AND MATERIAL

2.1 Preliminary Design of Quadcopter

The design of the quadcopter frame was based on several goal such as the ability to fly with a total weight (MTOW) of 5 kg, the flight time of 30 minutes, and a payload of 1.5 kg. The total motor thrust required was twice the weight of quadcopter, therefore the thrust required for each motor of 24.525 N (2.5 kg) [12]. According to the specifications of the motor available in the market, the maximum thrust can be achieved by using a 17-inch propeller and an electronic speed controller (ESC) with the specifications of 40A-6s. By considering the propeller

dimension, payload dimension and other electronic required, the frame of quadcopter is designed to have a wheelbase of 790 mm (the distance between motor centers). Therefore, it was capable of supporting 17-inch propellers with a clearance distance of approximately 126 mm between each propeller. Figure 1 shows a sketch of the quadcopter frame with a 790 mm wheelbase dimension.

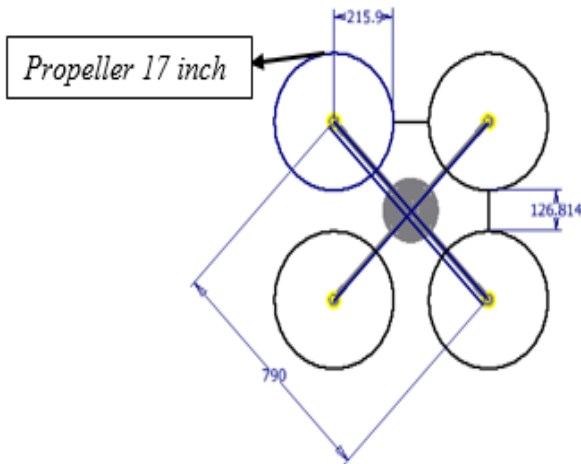


Figure1: Quadcopter frame sketch

2.2 Concept Design of the Quadcopter Frame

The quadcopter frame configuration was set using 'X' configuration. This configuration then was developed into three concept designs with variations of the central plate shape. The central plate shape was varied into three types: square (200 x 200mm), circular (diameter 200mm), and square with chamfer (200 x 200mm). Figure 2 shows three concept designs for the quadcopter that have been proposed. After obtaining several conceptual designs for the quadcopter frame, the next step was to proceed with selecting the best design using a decision matrix. It can be seen in Table 1, the decision matrix that was used.

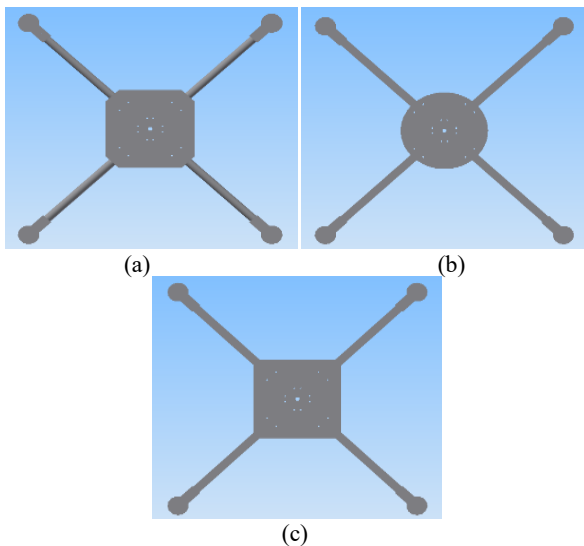


Figure2: Conceptual designs of quadcopter: (a) first concept, (b) second concept, (c) third concept

Table1: Decision matrix

Criteria	Weight (%)	Concept Design		
		1	2	3
Total mass	30	4	4	3
Drag Coefficient	40	3	4	3
Manufacturing process	30	3	3	3
Total	100	3.4	3.6	3.5

Total mass of quadcopter frame was calculated using 3d software design, taking into account the carbon fiber material for the frame. The carbon fiber has low density and high values of Ultimate Tensile Strength and Young's Modulus. These properties are best for applications where both strength and lightweight characteristics are important. The drag coefficient of central plate shape was estimated using table drag of simple shape [13]. From table 1, it can be shown that the second concept design has highest score so it will be selected as a design of quadcopter

2.3 MTOW and Flight Time Calculation

Once the selected design of frame is obtained, the calculations for the Maximum Take-Off Weight (MTOW) and flight time of the quadcopter aircraft can be conducted. For the motor and other electronic components, the mass can be obtained based on the data sheets provided of the product specifications. This approach ensures accurate weight estimation for the components of the quadcopter. Table 2 shows the results of the Maximum Take-Off Weight (MTOW) calculations for the quadcopter.

Table 2: MTOW calculation of quadcopter

Item	Specification	Mass (grams)
Frame	790 mm	563
Motor (4 pcs)	380 kv	592
Payload	Camera, gimbal etc.	1500
Battery	6s, 20000 mAh	2000
Propeller	17 Inch	60
ESC	40 A	180
Others	Nut, bolt, etc	100
Total		4995 grams

After obtaining the Maximum Take-Off Weight (MTOW) for the quadcopter, the flight time of the quadcopter can be calculated using Equation 1 and the given data, which includes a battery power. By assuming the quadcopter flies at a constant throttle of 65% (producing a thrust of 18 N/ motor) and consumes 226 watts of battery power, the calculated flight time is 33.4 minutes. It means that, under these conditions, the quadcopter can fly for approximately 33.44 minutes on the given battery capacity.

$$Flight\ time = 60 \times (Battery\ capacity / current\ draw) \quad (1)$$

2.4 Static Structural Calculation

After obtained the selected frame design, the next step is to conduct the static structural calculation in order to evaluate the strength of the frame to withstand loads twice the MTOW value. The materials used carbon fiber is defined in the calculation. The properties of the materials used in the quadcopter frame components are presented in Table 3.

Table3: Properties of the materials used for the quadcopter frame

Properties	Carbon fiber	Acrylic	PLA
Yield strength	475.13 MPa	200 MPa	340 Mpa
Young's modulus	16,671.12 MPa	2,760 MPa	3,500 Mpa
Poisson's ratio	0.1	0.34	0.38
Shear modulus	6,792 MPa	3000 MPa	1,200 MPa
Density	1.43 g/cm3	1.18 g/cm3	1.24 g/cm3

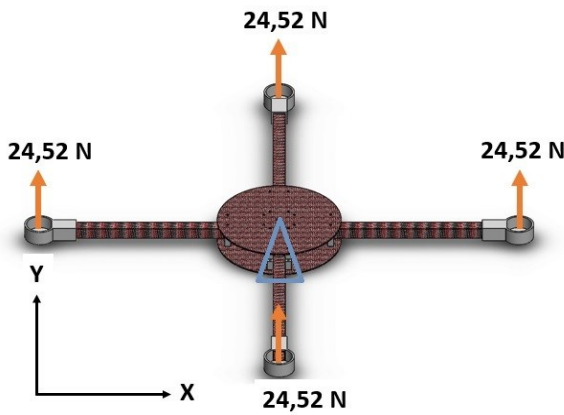


Figure 3: Loads and support on the quadcopter frame

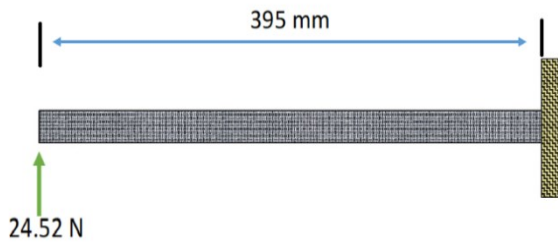


Figure 4: Physical model of quadcopter frame (arm)

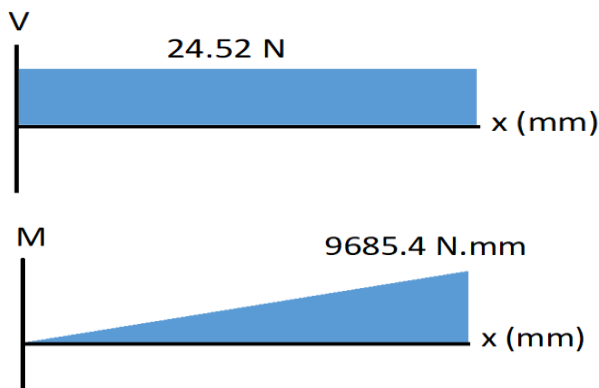


Figure 5: Shear force and bending moment in the quadcopter arm

Hinge supports are used at the center of the main plate (center of gravity) of the quadcopter. The working loads from the propulsion motor (24.525 N) was applied at the mounting motor as shown in Figure 3. By simplification of the quadcopter frame like beam, the physical model of quadcopter frame to be as shown Figure 4. By using Newton's first law, the results calculation of internal forces acting in the form of shear forces and bending moments along the beam are shown in Figure 5 [14].

The frame is the part of the quadcopter body, which supports all parts of the quadcopter. The frame is also used to place all components that are attached, so it can be properly integrated into the frame. The flight stability of the quadcopter is greatly affected by the strength and stress of the frame used. Frame deformation needs to be minimized so that the quadcopter remains stable, so it is necessary to calculate the stress that occurs in the frame. The shear stress and normal stress along the beam are calculated using the following equations [14].

$$\tau_{xy} = \frac{VQ}{It} \quad (2)$$

$$\sigma_x = \frac{My}{I} \quad (3)$$

Subsequently, the maximum stress is calculated using the following equation.

$$\sigma_{average} = \frac{\sigma_x + \sigma_y}{2} \quad (4)$$

$$R = \sqrt{(\sigma_x - \sigma_{average})^2 + \tau_{xy}^2} \quad (5)$$

$$\sigma_1 = \sigma_{average} \pm R \quad (6)$$

The results of these calculations represent the maximum stress acting on the quadcopter arm. The maximum stress operates at the point around the clamp support connecting the central plate and the arm of the quadcopter. Next, the deflection values along the arm are calculated using the following equation [14].

$$v = \frac{Px^2}{6EI} (3L - x) \quad (7)$$

2.5 The Quadcopter Frame Manufacturing Process

There are several components of the quadcopter to be manufactured: the main plate, arms, clamps, and motor mountings. The manufacturing process of quadcopter arms begins with creating its molds. The molds are made using fiberglass material and polyester resin. The arm model is derived from a 20 mm x 20 mm aluminum rod with a length of 50 cm. This model is then fitted with melamine plywood as a divider in the middle. To prevent the mold surface from sticking to the fiberglass, a waxing process is carried out on the model's surface four times, with a 10-minute interval between each application. Then, the waxed model is coated with 150 grams of gelcoat, 0.75 ml of cobalt, 3 ml of catalyst, and 7.5 grams of color pigment. This mold is made using five layers of fiberglass. The completed mold is then used for manufacturing of the quadcopter arms. It is carried out using carbon fiber material and epoxy resin with the vacuum bagging method.

Figure 6 shows the manufacturing process of the quadcopter arms.



Figure 6: The manufacturing process of the quadcopter arms

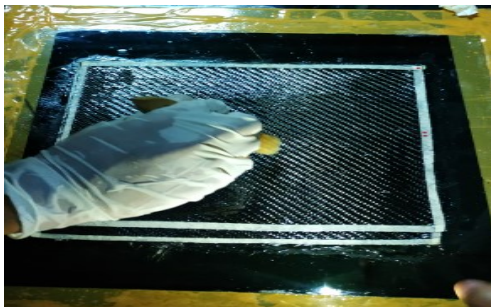


Figure 7: The manufacturing process of main plate



Figure 8: The 3d printing process of motor mounting

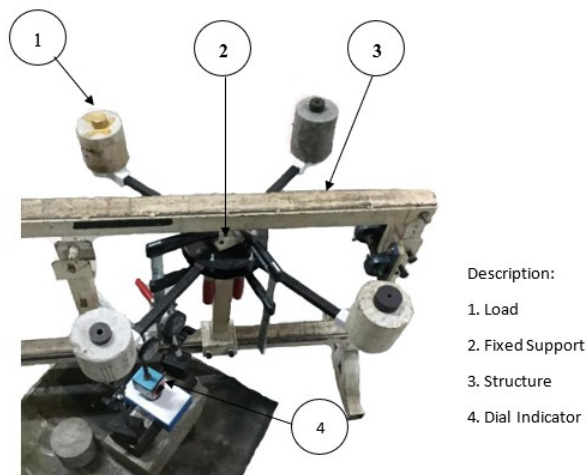


Figure 9: The setup for the quadcopter frame deflection measurement

The manufacturing process of the main plate is similar to the process of quadcopter arms. However, the mold used consists of two glass sheets. Figure 7 shows the manufacturing process of main plate. The motor mounting design is created in three dimensions and converted into STL format. The file is then loaded into the 3D printer with a nozzle temperature setting of 200°C. Next, for the clamp component, acrylic material is used, which is cut according to the design. The cutting process is carried out using a grinding machine, after which the acrylic is drilled using a drill machine for bolt installation. Figure 8 shows the 3d printing process of motor mounting.

The assembly process begins with the assembly of the central plate and arms. The four arms and two central plates made from carbon fiber are assembled using bolts, nuts, and washers. The motor mounts are also assembled using bolt and nut connections. After the quadcopter frame is fully assembled, its dimensions and mass are measured. The measurement results will be compared with the design specifications.

2.6 The Deflection Measurement of Quadcopter Frame

The deflection measurement is conducted using the setup equipment as shown in Figure 9. The actual deflection will be compared to the calculated deflection. The deflection measurement equipment consists of a supporting structure, the quadcopter frame, and a dial indicator [15]. The measurement is conducted at six points along the quadcopter arms using three dial indicators. The measurement starts from the motor mounting end, with each testing point spaced 5 cm apart. The testing conditions are adjusted while the quadcopter is in flight. During flight, the motors exert an upward force on the arms. Therefore, during the quadcopter frame testing, it is inverted to simulate the actual conditions during flight. For support, the quadcopter frame is clamped at the center of the plate. The load (2.5 kg) applied to the quadcopter frame is placed on the motor mounting. Figure 9 shows the setup for the quadcopter frame deflection measurement.

3.0 RESULTS AND DISCUSSION

3.1 Results of the Quadcopter Frame Design and Manufacturing

Figure 10-11 shows the Result of Quadcopter Frame Design and Manufacturing.



Figure 10: Design result of quadcopter frame

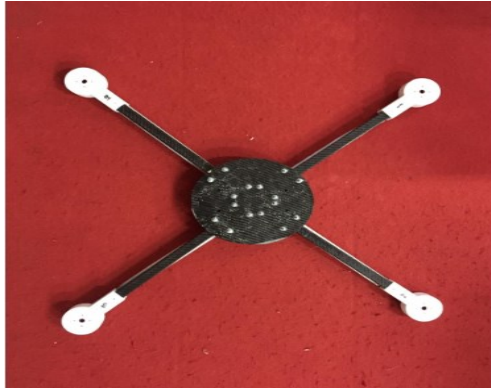


Figure 11: Manufacturing result of quadcopter frame

After the quadcopter frame is constructed, the dimensions and mass of the quadcopter frame are compared to the design dimensions of the quadcopter as shown in Table 4. From Table 4, it can be seen that the actual dimensions of the quadcopter frame was compared to the design dimension has no different significantly. Dimensionally, the quadcopter frame can be considered to be in accordance with the design. After measuring the dimensions of the quadcopter frame, the mass of each component of the quadcopter frame is then weighed. Table 5 shows the design and the actual mass of the quadcopter frame.

Table 4: The design and the actual dimensions of the quadcopter frame

Parts	Design dimensions	Actual Dimension
Wheelbase	790	793
Arm	355x20x1	356x20x1.1
Plat Tengah	D 200 t 2	D 200 t 2.1
Acrylic	35x10x35	36x10x35
Mounting Motor	85 x 50	85 x 50

Table 5: The design and the actual mass of the quadcopter frame

Parts	Qty	Design mass (grams)	Actual mass (grams)
Arms	4	152	165
Center plate	2	186	190
Clamp	8	96	110
Mounting Motor	4	124	130
Total mass		563	595

Based on Table 5, the difference between the actual mass and the design mass is 32 grams. It occurs due to several factors, such as an excess of resin during the frame's production, and resin absorption during the vacuum process is uneven.

3.2 Structural Strength Calculation and Test Result

From Figure 12, it can be observed that the maximum stress occurs at the fixed support of the beam (21.17 MPa). It is in line with the cantilever beam principle, where the highest stress occurs at the support area [14].

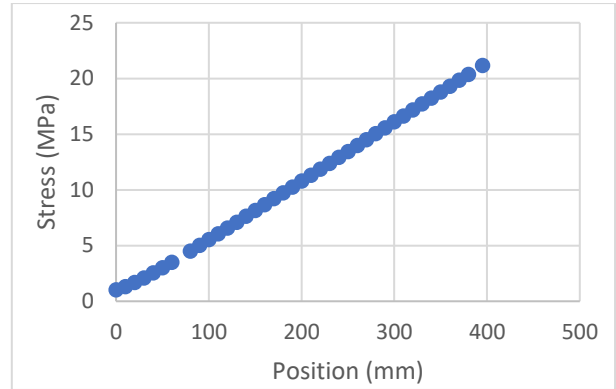


Figure 8: The stress distribution along the quadcopter frame

The frame structure of the quadcopter is considered safe when it can withstand the load from the motors if the safety factor value is greater than 1.5. To validate the safety of the frame structure, the safety factor is calculated using Equation 8.

$$Safety\ factor = \frac{Yield\ Strength}{Working\ Stress} \quad (8)$$

From the calculation, the safety factor value of 22.44 is obtained. It indicates that the quadcopter frame is in a safe condition because its safety factor value is greater than 1.5. Figure 13 to Figure 15 show the distribution of the actual deflection and the calculated deflection of quadcopter arms.

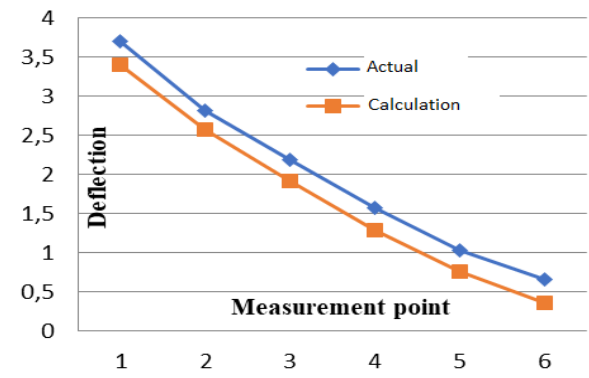


Figure 13: The distribution of the first arm deflection (right-front)

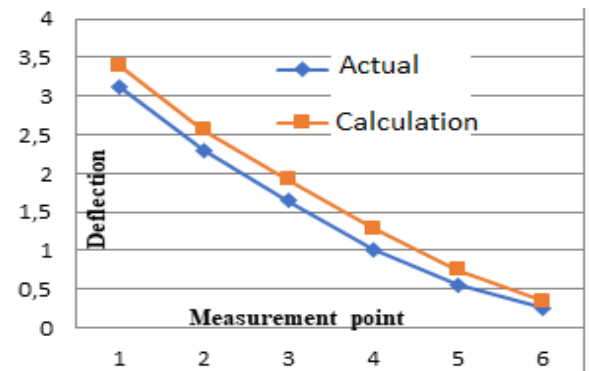


Figure 14: The second arm distribution deflection (left-front)

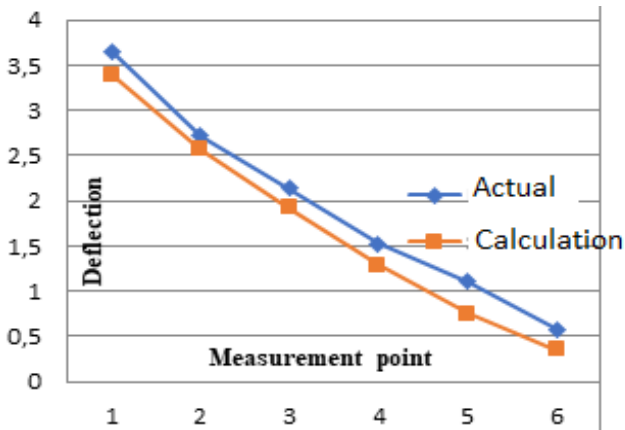


Figure 15: The distribution of the third arm deflection (right-rear)

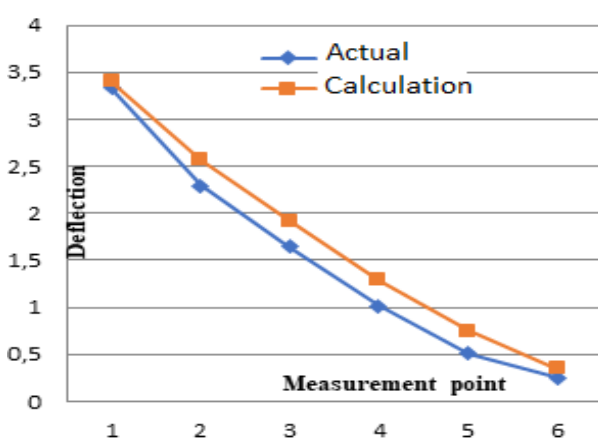


Figure 16: The distribution of the fourth arm deflection (right-rear)

In general, the actual deflection distribution that occurs has a trend similar to the calculated deflection distribution. The maximum deflection that occurs is around 3.7mm. It occurs as the quadcopter frame subjected to the maximum thrust from the propulsion system. It indicates that the deflection value is still within a safe range.

From Figure 13-16, it can be observed that the actual deflection of each arm has slightly different. It shows that the production results of each arm have slightly different material properties. It occurs due to the vacuum bagging process, where the excess resin absorbed by the peel ply fabric is uneven. However, in general, the differences that occur are not significantly large (below 1 mm), so the production results of the quadcopter frame can be considered correspond to the design. The results of the calculation of structural strength and deflection tests show that the quadcopter frame can be developed further into a quadcopter platform that has an MTOW of 5 kg and capable of carrying payload of 1.5 kg.

CONCLUSION

The selected design of the quadcopter frame has the following

specifications: the central plate is circular in shape, the wheelbase dimension is 790 mm, and the weight is 563 grams. The prototype of the quadcopter frame has been successfully constructed according to the design, with a wheelbase dimension of 793 mm and a weight of 595 grams. The calculation showed the maximum stress of 21.17 MPa, and a safety factor of 22.44. Therefore, it can be stated that the quadcopter frame is in a safe condition. The actual deflection has a trend similar to the calculated deflection distribution without significantly different.

ACKNOWLEDGMENT

This research was supported by LPPM, Universitas Riau.

REFERENCES

- [1] Tyan, M., Van Nguyen, N., Kim, S., & Lee, J. W. (2017). Comprehensive preliminary sizing/resizing method for a fixed wing-VTOL electric UAV. *Aerospace Science and Technology*, 71, 30-41. doi: 10.1016/j.ast.2017.09.008.
- [2] Asral, Kaspul Anuar, & Agung Soegihin. (2022). Aerodynamic Analysis of Unnamed Aerial Vehicle Serindit V-2 Using Computational Fluid Dynamics. *Journal of Advanced Research in Fluid Mechanics and Thermal Sciences*, 93(1), 83-93. <https://doi.org/10.37934/arfmts.93.1.8393>
- [3] Golui, D.K., Pradhan, N., Tudu, S.M. & Anjumol, K.S. (2019). Detailed Design of a Tail-Sitter. Report Project, 1-76, Depart. of Aerospace Engineering Indian Institute of Space Science and Technology Thiruvananthapuram. doi: 10.13140/RG.2.2.10704.87045.
- [4] Anuar, K., Fatra, W. & Akbar, M. (2020). Tricopter vehicle frame structure design integrated as platform of fixed wing atha mapper 2150. *Journal of Ocean, Mechanical and Aerospace -Science and Engineering-*, 64(2), 68-72. doi:10.36842/jomase.v64i2.218.
- [5] Anuar, K., Fatra, W., Akbar, M., Nazaruddin, N., Syafri, S., Sari, A.W., & Utama, R.R. (2023). Design and aerodynamic analysis of fixed-wing vertical take-off landing (fw-vtol) uav. *Journal of Advanced Research in Fluid Mechanics and Thermal Sciences*, 106(1), 136-146.
- [6] Jetley, P., Sujit, P. B. & Saripalli, S. (2017). Safe landing of fixed wing UAVs. In *2017 47th Annual IEEE/IFIP International Conference on Dependable Systems and Networks Workshops (DSN-W)*, 2-9, IEEE. doi: 10.1109/DSN-W.2017.43.
- [7] Anuar, K. & Herisiswanto (2019). Desain perangkat hight lift device (hld) guna meningkatkan koefisien gaya angkat pada sayap wahana terbang uav serindit v-1. *Multitek Indonesia*, 13(1), 9-15. doi: 10.24269/mtkind.v13i1.1736
- [8] Avanzini, G., Di Nisio, A., Lanzolla, A.M.L. & Stigliano, D. (2020). A test-bench for battery-motor-propeller assemblies designed for multirotor vehicles. In *2020 IEEE 7th International Workshop on Metrology for AeroSpace (MetroAeroSpace)*, 600-605). IEEE. doi: 10.1109/MetroAeroSpace48742.2020.9160320.
- [9] Anuar, K. & Akbar, M. (2019). Wing design of uav serindit v-1. In *IOP Conference Series: Materials Science*

- and Engineering, 539(1), 012002. IOP Publishing. doi: 10.1088/1757-899X/539/1/012002.
- [10] Yu, S. & Kwon, Y. (2017). Development of VTOL drone for stable transit flight. *Journal of Computer and Communications*, 5(7), 36-43. doi: 10.4236/jcc.2017.57004.
- [11] Anuar, K., Akbar, M., Aziz, H.A., & Soegihin, A. (2022). Experimental test on aerodynamic performance of propeller and its effect on the flight performance of serindit v-2 uav. *Journal of Advanced Research in Fluid Mechanics and Thermal Sciences*, 91(2), 120-132. doi: 10.37934/arfmts.91.2.120132.
- [12] Das, H., Baskaran, V. & Arya, H. (2016). Static performance analysis of electric propulsion system in quadrotors. In *2016 International Conference on Control, Instrumentation, Communication and Computational Technologies (ICCICCT)*, 495-500. IEEE. doi: 10.1109/ICCICCT.2016.7988001.
- [13] Mohammed, M.G., Messerman, A.F., Mayhan, B.D. & Trauth, K.M. (2016). Theory and practice of the hydrodynamic redesign of artificial hellbender habitat. *Herpetological Review*, 47(4), 586-591.
- [14] Hibbeler, R.C. (2011). *Mechanics of Materials*, Eight Edd, Prentice Hall.
- [15] Teguh, M.T., Anuar, K., Taslim, M. & Saputra, R.G. (2019). The application of empty palm fruit bunch (epfb) as a material for fixed wing type unmanned aerial vehicle fuselage production. *Journal of Ocean, Mechanical and Aerospace-science and engineering*, 63(3), 13-16. doi: 10.36842/jomase.v63i3.133.